Figure Captions

Figure 11. Sedimentation curves at Sites 1115 (solid line), 1109 (dashed line), 1118 (dotted line), 1108 (solid line upper right), 1114 (dashed line upper right), and 1116 (dotted line upper right), based on nannofossil (square) and planktonic foraminifer (circle) datum events, magnetic chron and subchron boundaries (triangle), and lithostratigraphic correlation (star). Symbols with arrows denote actual datum point can be above or below and older or younger than indicated by the symbols. Shown below are average sedimentation rates, calculated for intervals separated by vertical lines, and paleobathymetry, based on benthic foraminifers, at Sites 1115, 1109, and 1118. Broken lines indicate uncertainty in the placement of paleodepth boundaries. Unconformity represented by wavy line.

Figure 12. Calcium carbonate content plotted vs. depth at Site 1115. Note the downward decrease in carbonate content to 400 mbsf.

Figure 13. Digital photomicrograph. Plane-polarized light. Crystal vitric tuff, with abundant angular, fresh pipe vesicle glass shards in a glassy matrix (Sample 180-1118A-38R-3, 128–130 cm).

Figure 14. Digital photomicrograph. Plane-polarized light. A pumiceous rock containing phenocrysts of hornblende within a glassy groundmass. Occurs as a granule-size clast within a sandy silty claystone (Sample 180-1108B-12R-5, 50–53 cm).

Figure 15. Digital photomicrograph. Viewed under crossed nicols. A well-rounded clast of fresh glassy basalt with plagioclase and biotite microphenocrysts, set in a calcitic matrix including volcanic and metamorphic grains (Sample 180-1115C-12R-4, 144–148 cm).

Figure 16. Digital photomicrograph. Viewed under crossed nicols . A subrounded clast of basalt with plagioclase microphenocrysts (right); an acidic clast (left), and a clast of serpentinite (lower). The matrix is calcareous, with quartz and feldspar grains (Sample 180-1108B-3R-CC, 0–4 cm).

Figure 17. Correlated lithologic logs of Sites 1114, 1116, and 1117 from the footwall of the Woodlark rift basin. See site summaries for discussion.

Figure 18. Digital photomicrograph. Angular fragment of calc-schist, surrounded by glassy basalt and silicic fragments, set in a sparry calcite cement (Sample 180-1116A-13R-2, 25–27 cm).

Figure 19. Occurrence of volcanogenic ash layers at Sites 1118, 1109, and 1115 shown in terms of thickness (gray pattern) and number of volcanogenic ash layers (black pattern) for Pliocene–Pleistocene time. Note: the spiky nature of the peaks of volcaniclastic input are in part artifacts of variable core recovery. Refer to the visual core descriptions on the CD-ROM for details of recovery.

Figure 20. Physical properties data for Sites 1108, 1109, 1111, 1114, 1115, 1116, and 1118. **A.** Porosity data, as measured from discrete index property samples. Dashed lines show the depth of the regional unconformity at the northern sites. **B.** Porosity data, with depth shifts as follows: Site 1108: 500 m added to mbsf depths above 165 mbsf (the location of a fault zone), 700 m added below 165 mbsf; 750 m added to Site 1114 data; and 1000 m added to Site 1116 data. Data below the unconformities at Sites 1109, 1115, and 1118 are not shown because of the unknown hiatus. See text for discussion.

Figure 21. Magnetic susceptibility for Sites 1118, 1109, and 1115 aligned with respect to the location of the Top Mammoth datum (interpolated from biostratigraphy at Site 1109).

Figure 22. Magnetic susceptibility for Sites 1118, 1109, and 1115 plotted as a function of time. Given the accuracy of the age data, the transition from low-amplitude to high-amplitude magnetic susceptibility is approximately coeval across the sites.

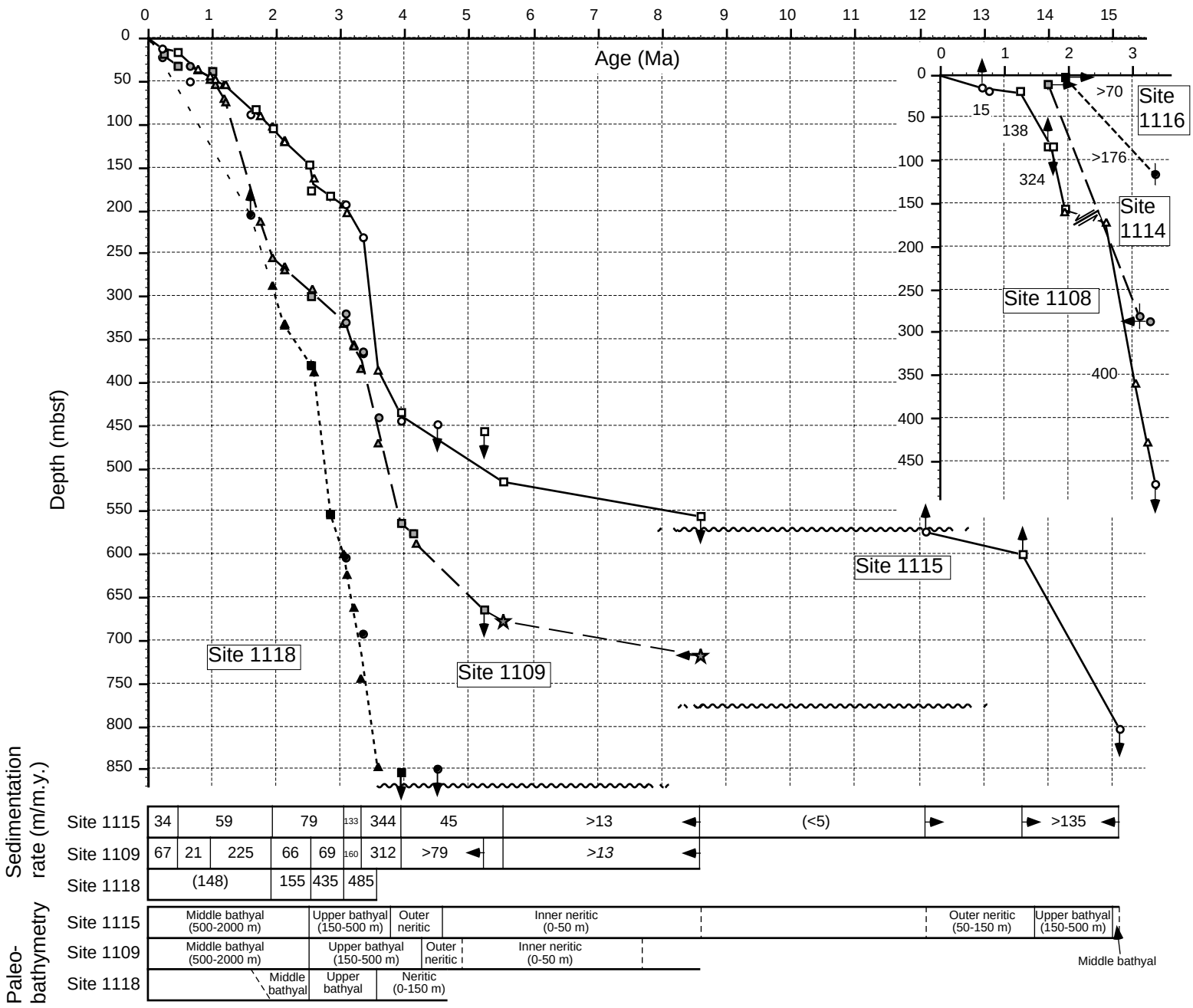
Age (Ma)
Depth (mbsf)
Site 1118
Site 1109
Site 1115
Site 1108
Site 1114
Site 1116
15
138
324
>70
>176
400
Sedimentation rate (m/m.y.)
Site 1115
34
59
79
133
344
45
>13
(<5)
>135
Site 1109
67
21
225
66
69
160
312
>79
>13
Site 1118
(148)
155
435
485
Paleo-bathymetry
Site 1115
Middle bathyal (500-2000 m)
Upper bathyal (150-500 m)
Outer neritic
Inner neritic (0-50 m)
Outer neritic (50-150 m)
Upper bathyal (150-500 m)
Site 1109
Middle bathyal (500-2000 m)
Upper bathyal (150-500 m)
Outer neritic
Inner neritic (0-50 m)
Middle bathyal
Site 1118
Middle bathyal
Upper bathyal
Neritic (0-150 m)

Figure 11

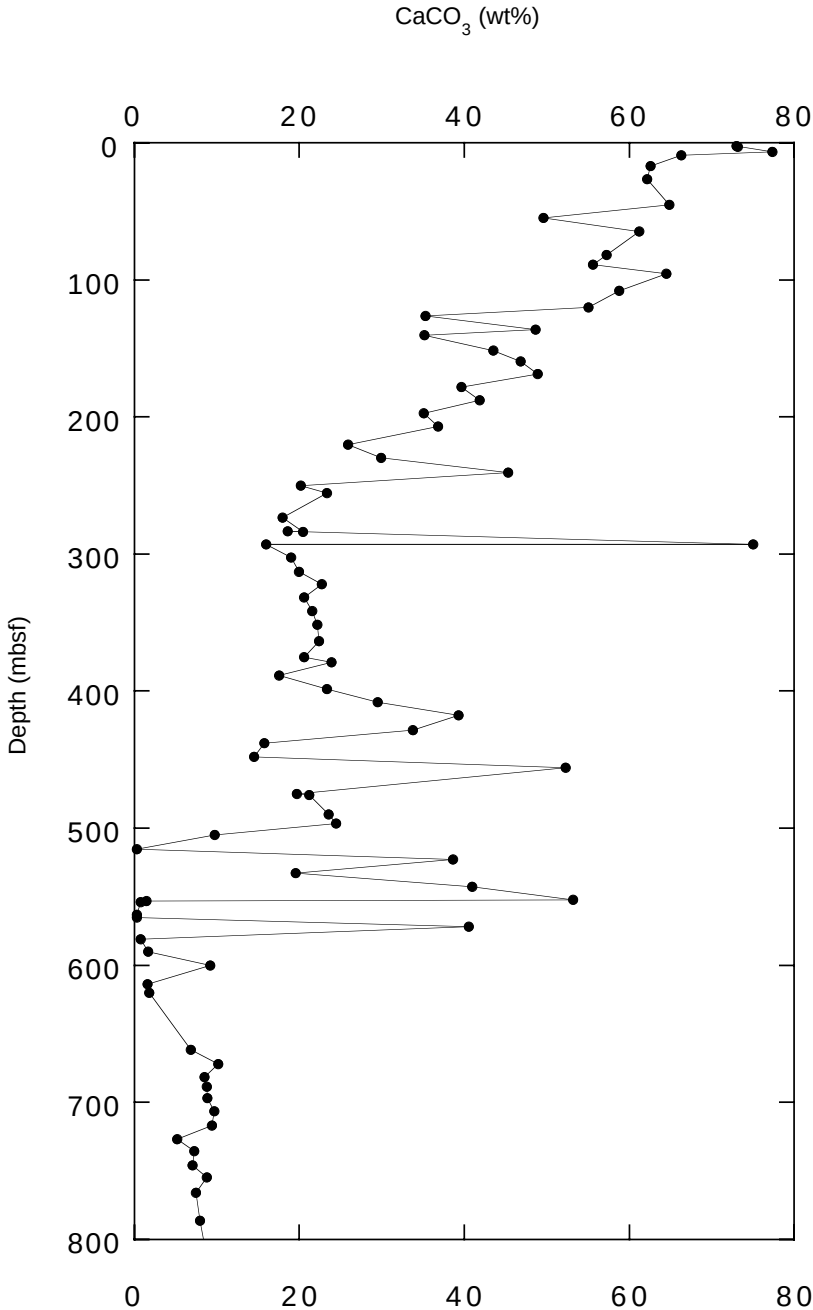
CaCO3 (wt%)
0
20
40
60
80
Depth (mbsf)
0
100
200
300
400
500
600
700
800

Figure 12

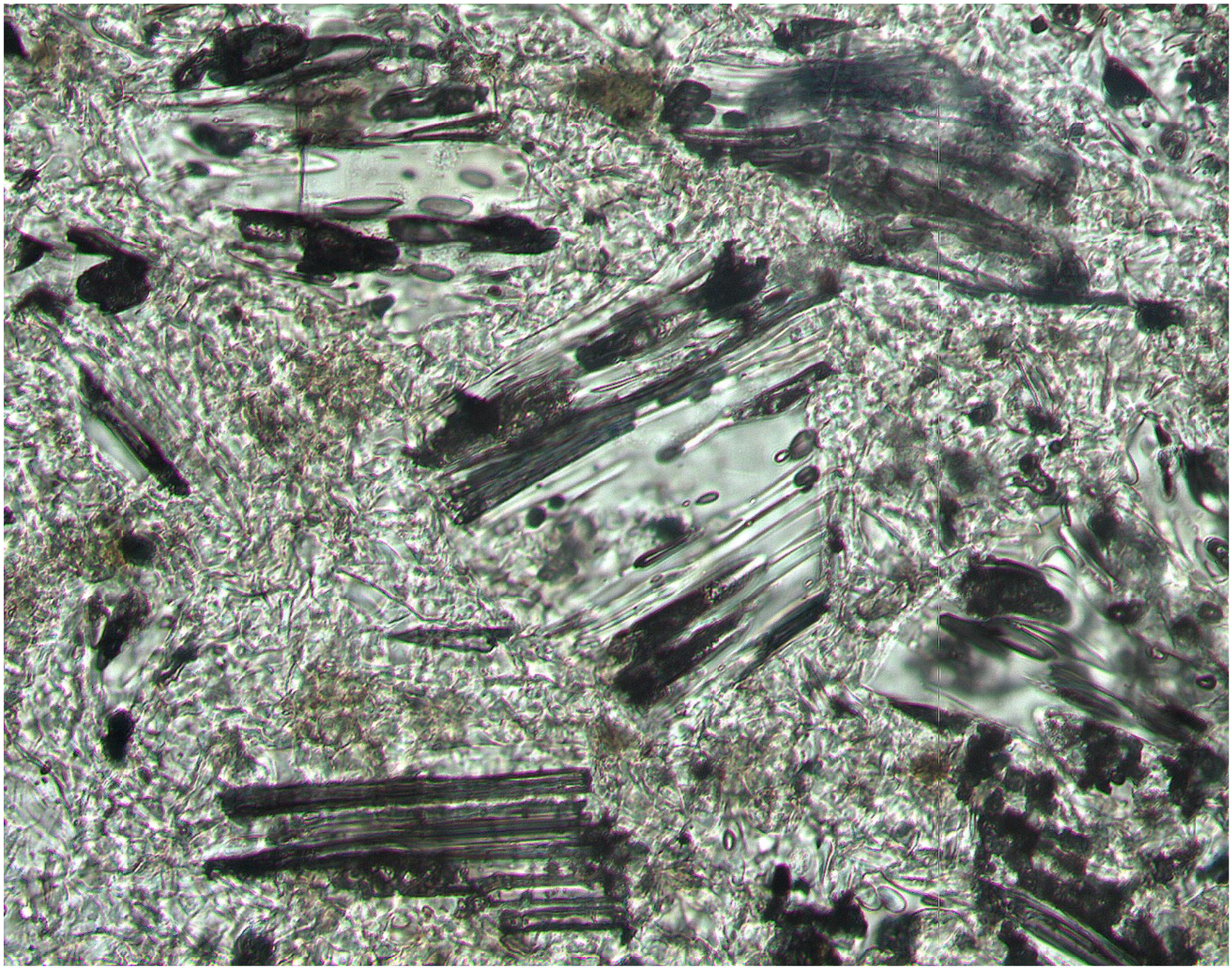

Figure 13

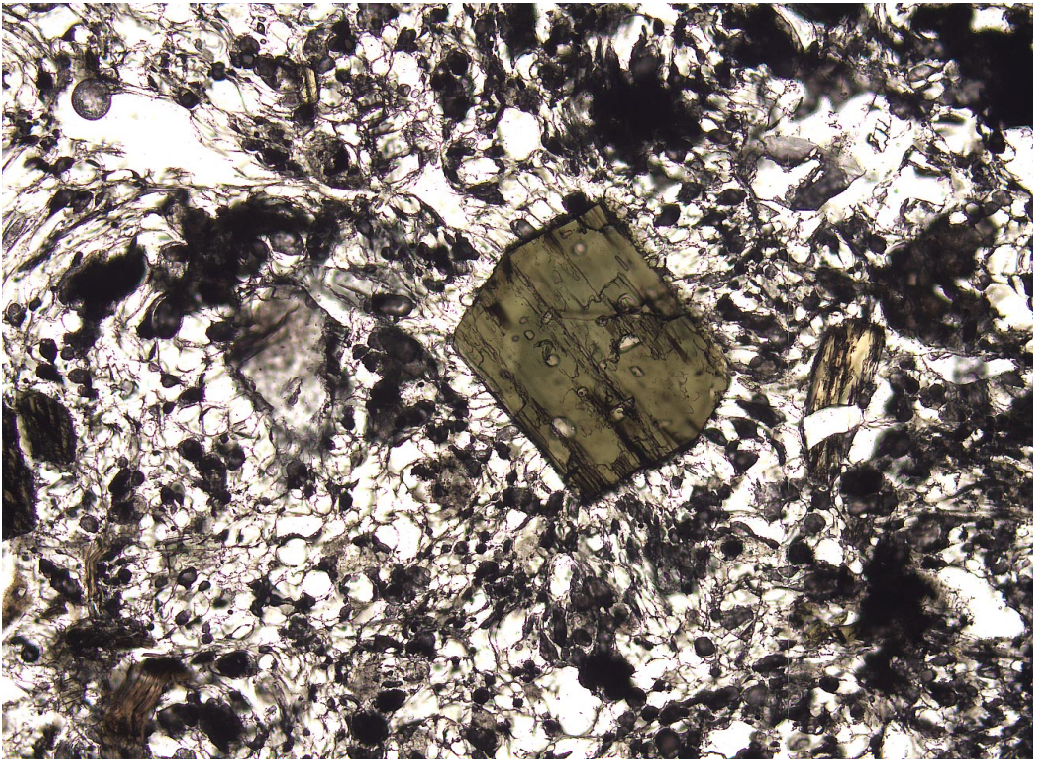

Figure 14

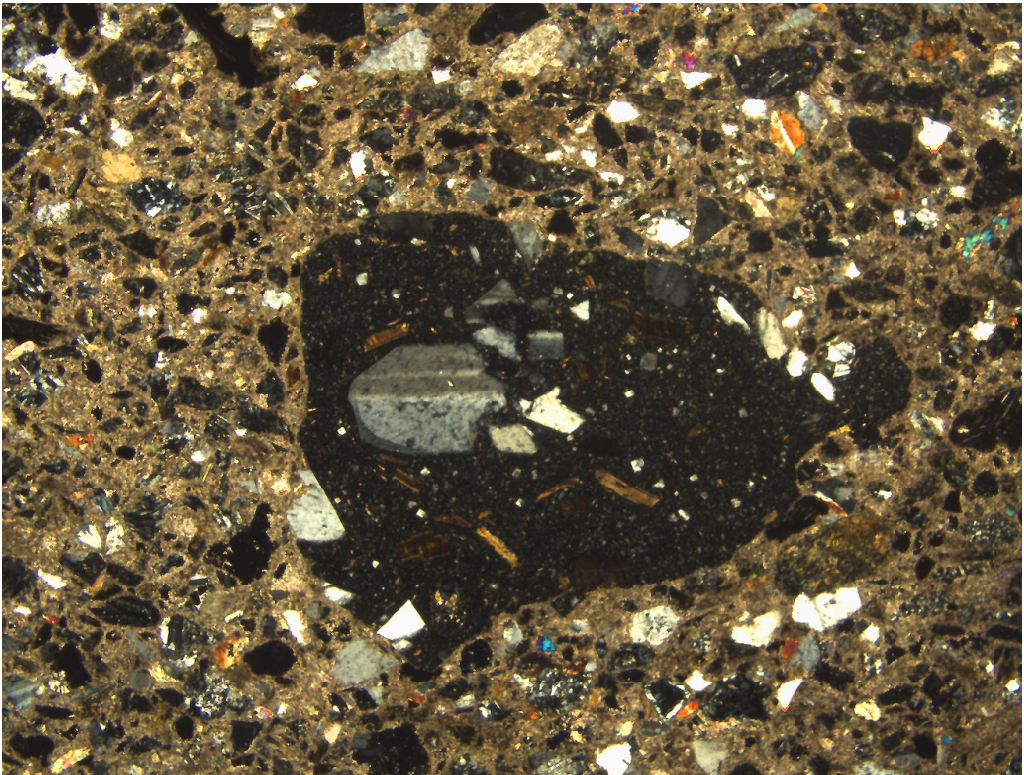

4 mm

Figure 15

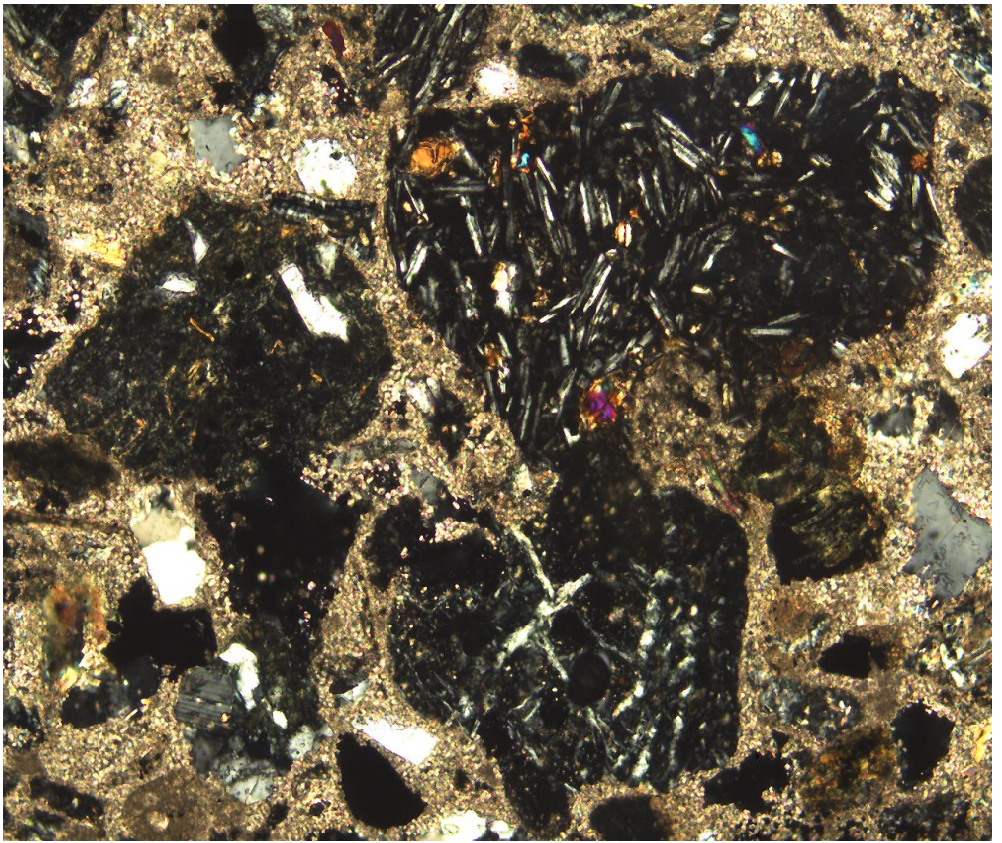

Figure 16

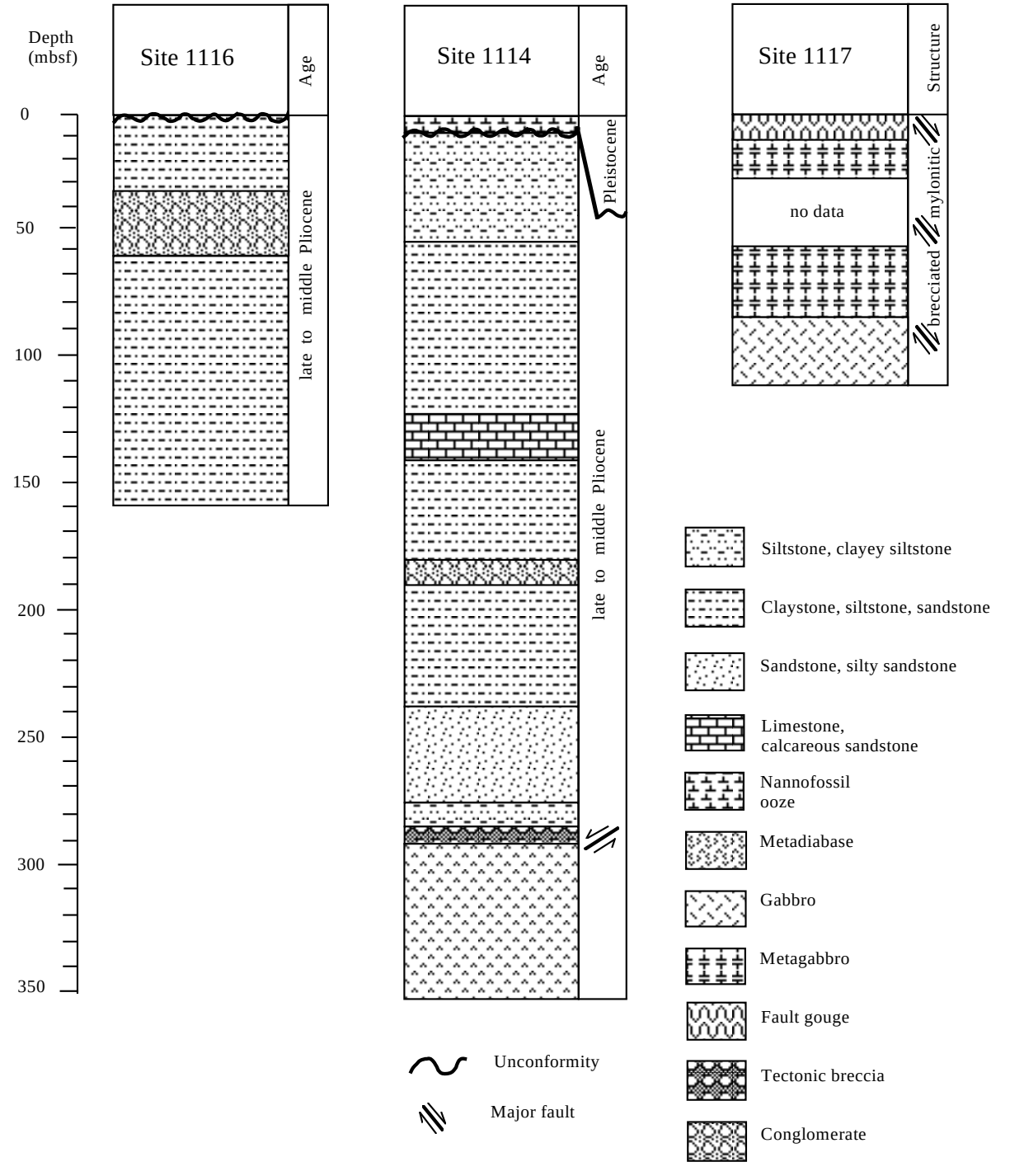
Depth
(mbsf)
0
50
100
150
200
250
300
350
Site 1116
Age
late to middle Pliocene
Site 1114
Age
Pleistocene
late to middle Pliocene
Site 1117
Structure
no data
mylonitic
brecciated
Siltstone, clayey siltstone
Claystone, siltstone, sandstone
Sandstone, silty sandstone
Limestone,
calcareous sandstone
Nannofossil
ooze
Metadiabase
Gabbro
Metagabbro
Fault gouge
Tectonic breccia
Conglomerate
Unconformity
Major fault

Figure 17

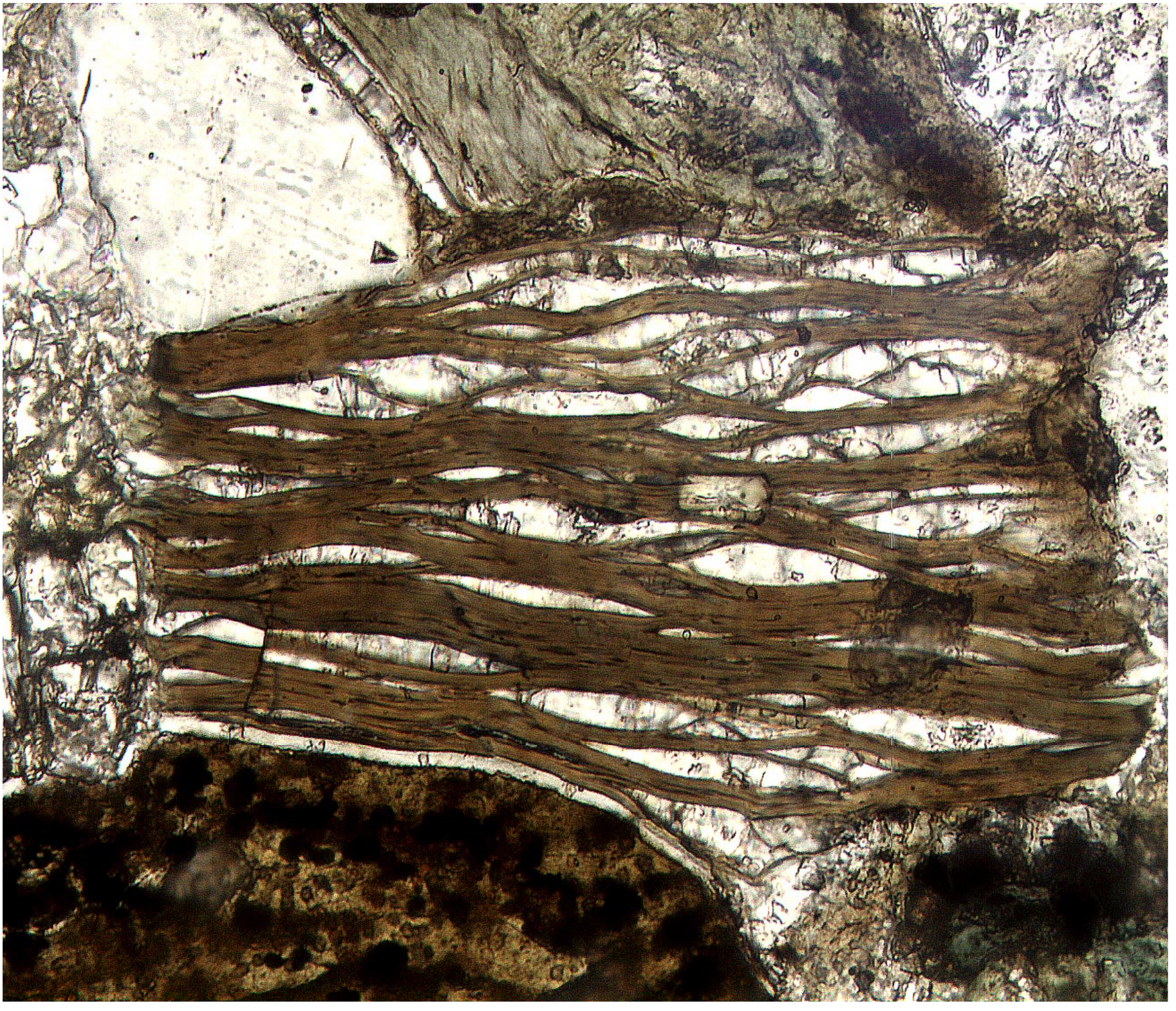

0.25 mm

Figure 18

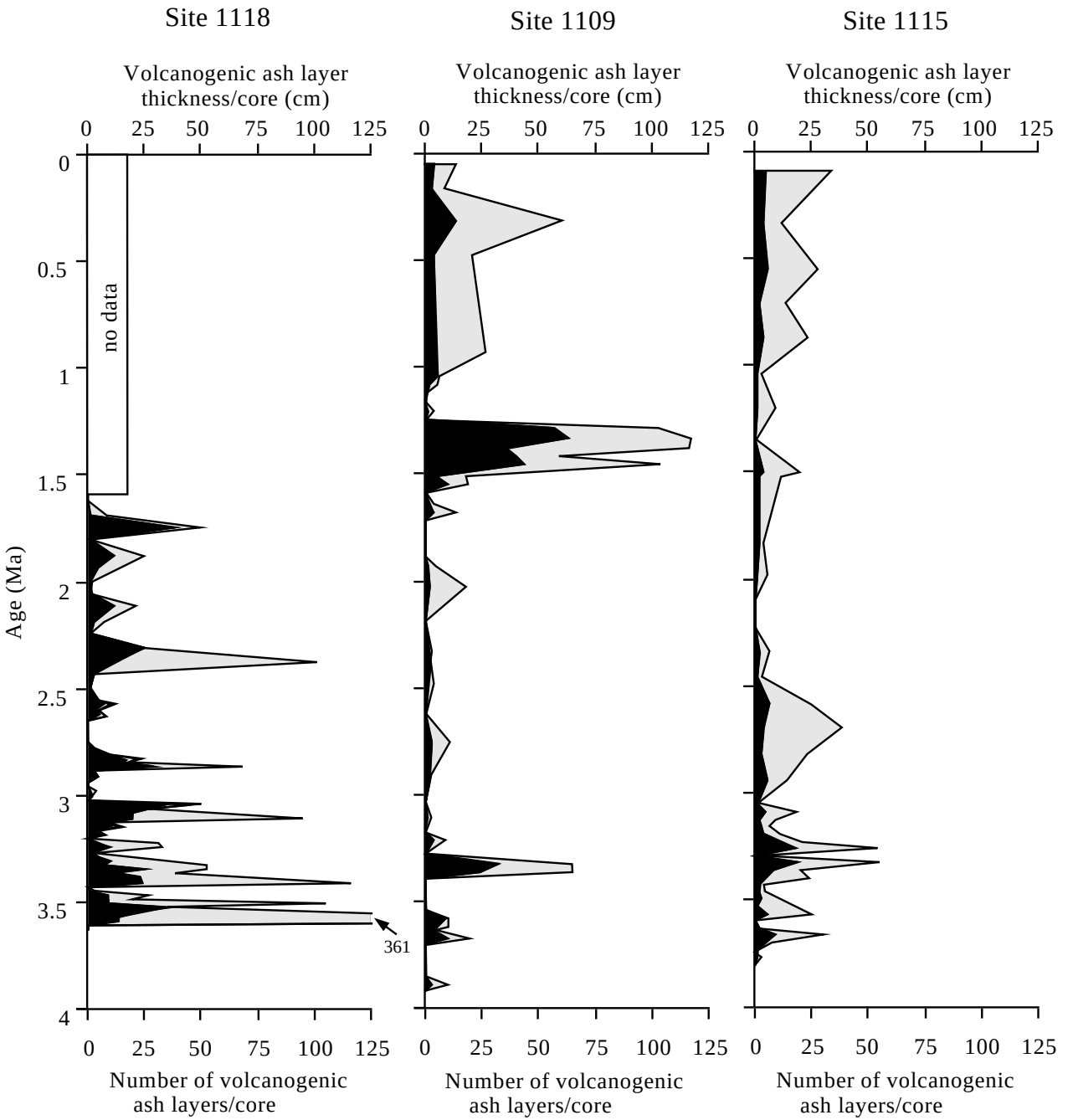
Site 1118
Site 1109
Site 1115
Volcanogenic ash layer thickness/core (cm)
0 25 50 75 100 125
no data
Age (Ma)
0
0.5
1
1.5
2
2.5
3
3.5
4
361
Number of volcanogenic ash layers/core

Figure 19

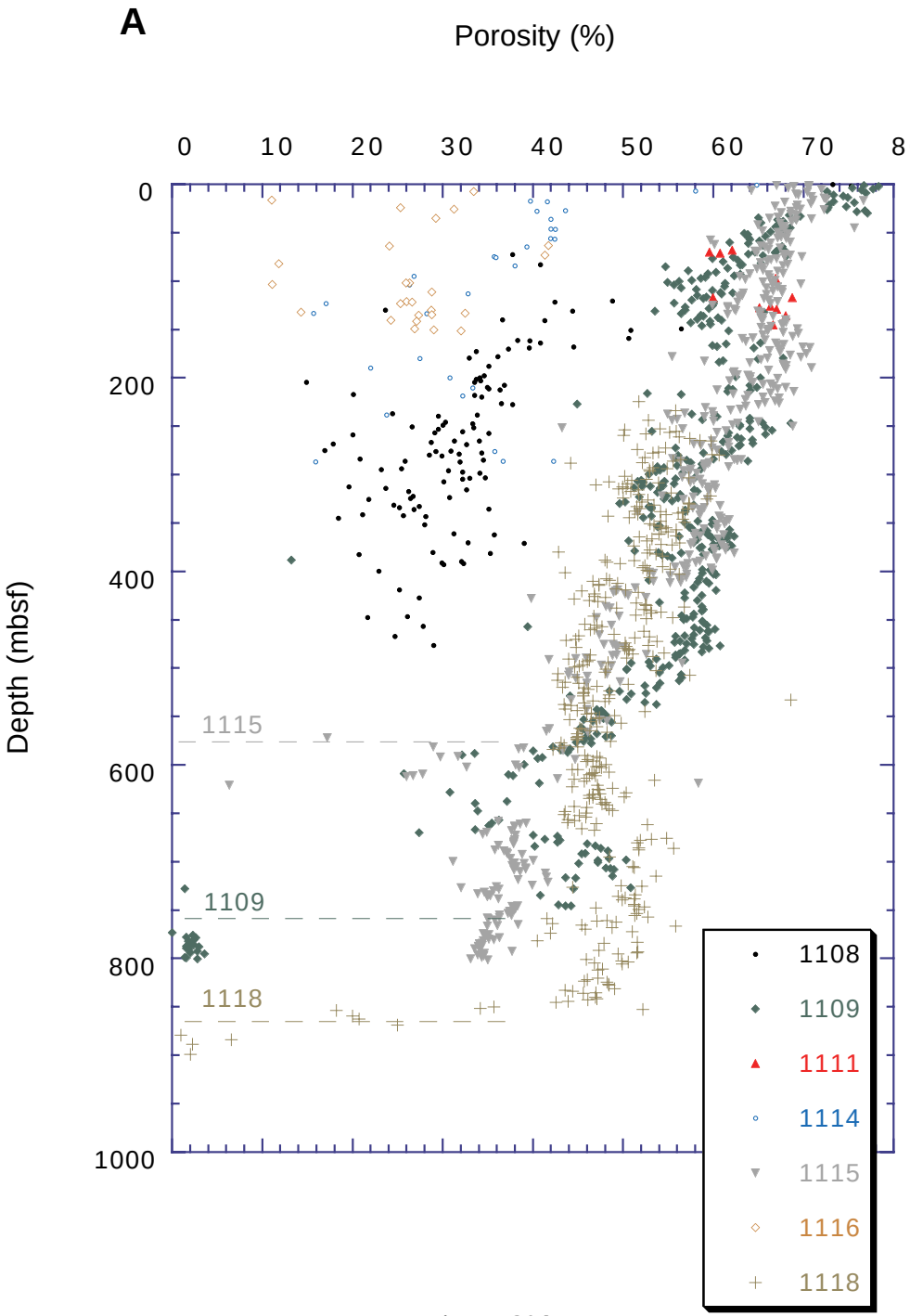
A
Porosity (%)
0
10
20
30
40
50
60
70
80
Depth (mbsf)
0
200
400
600
800
1000
1115
1109
1118
1108
1109
1111
1114
1115
1116
1118

Figure 20A

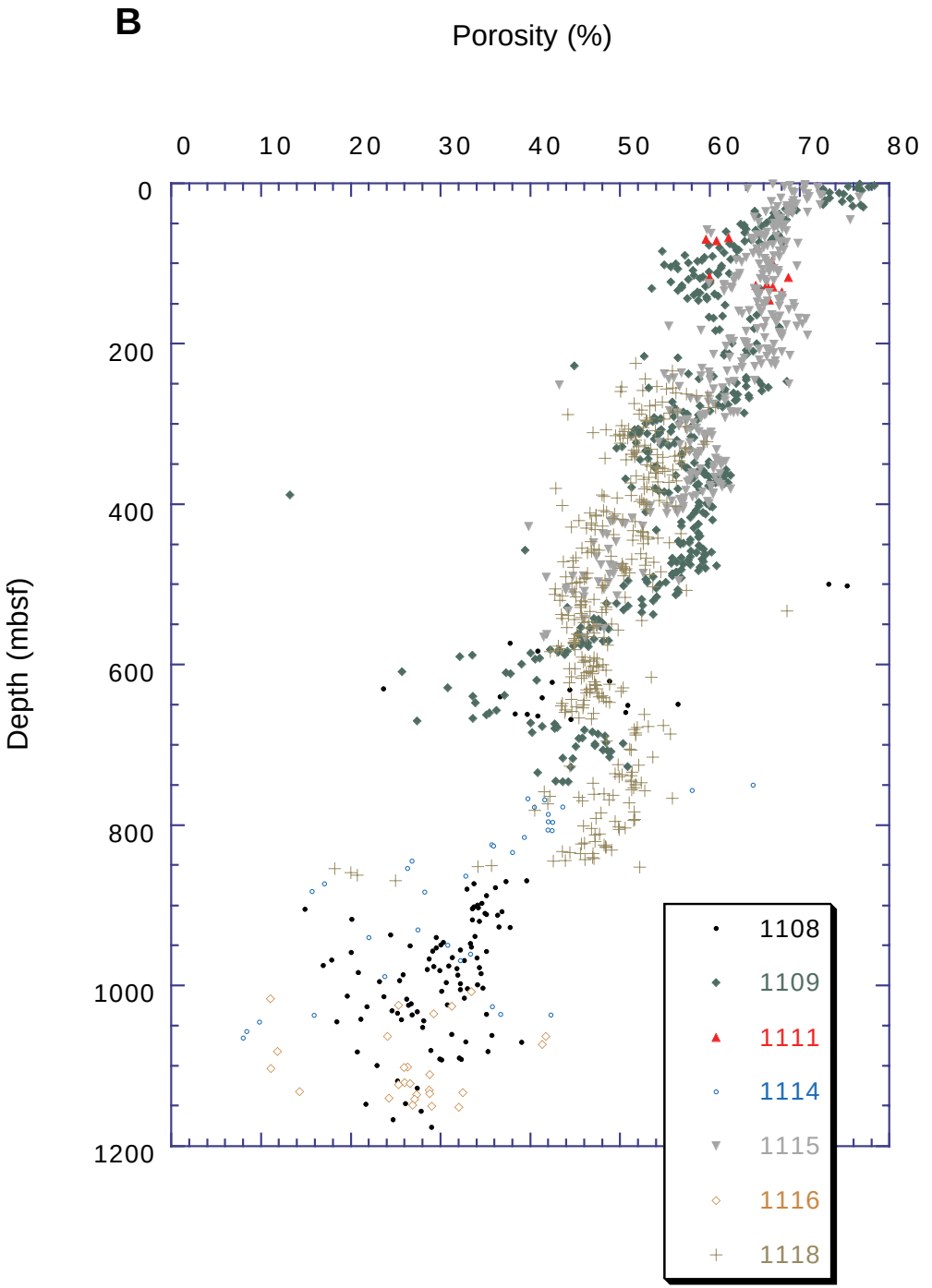
B
Porosity (%)
0
10
20
30
40
50
60
70
80
Depth (mbsf)
0
200
400
600
800
1000
1200
1108
1109
1111
1114
1115
1116
1118

Figure 20B

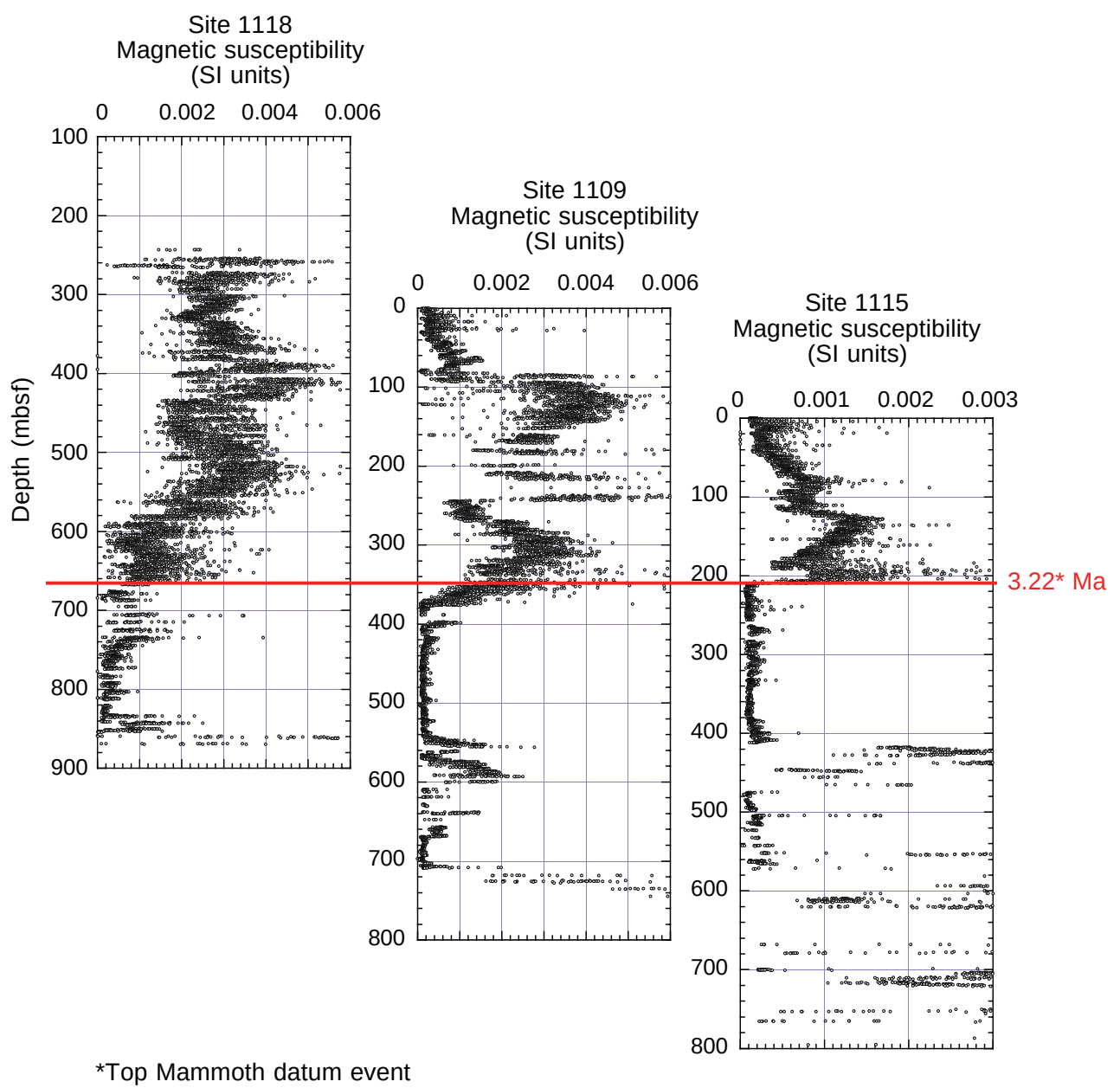

*Top Mammoth datum event

Figure 21

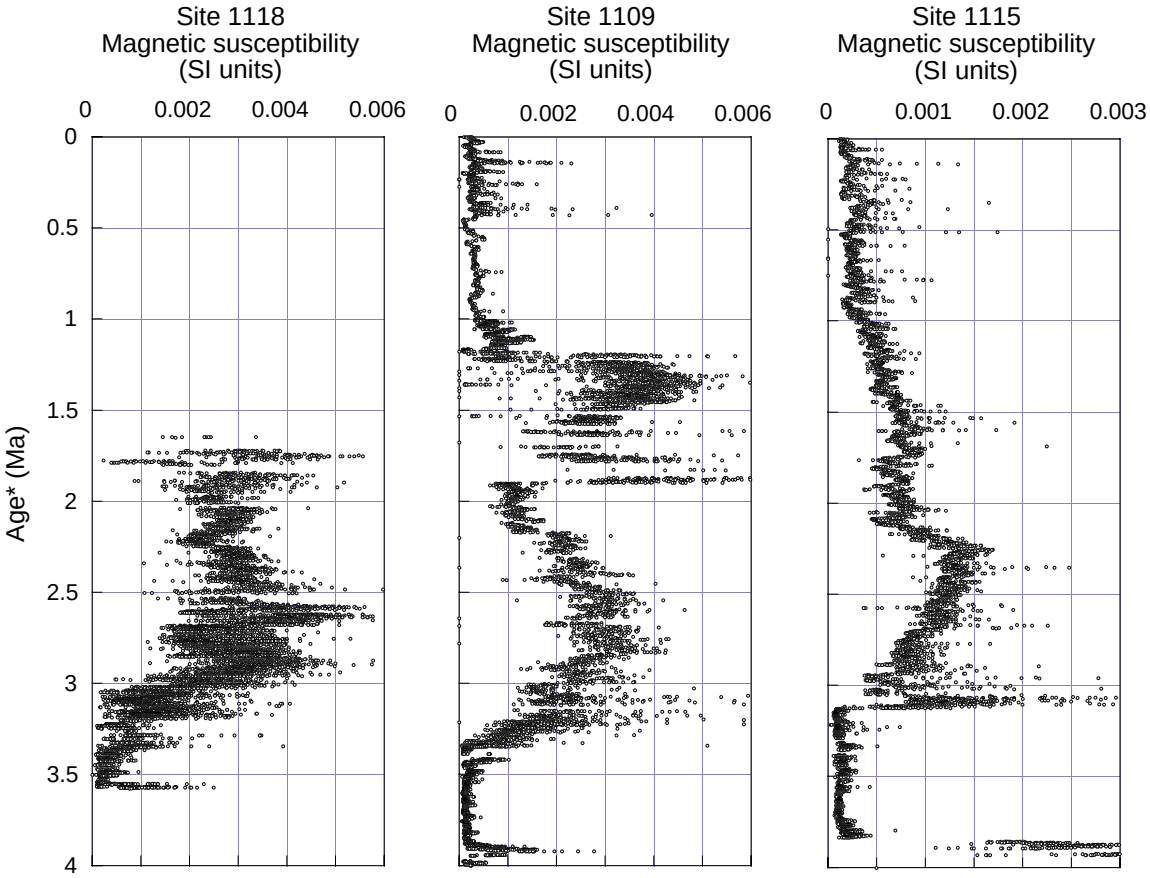

*Biostratigraphic/paleomagnetic estimates

Figure 22